Mössbauer study of the magnetic character and ordering process of the cubic γ-$FeSi_2$ phase obtained by Fe implantation into a Si(100) matrix

R. L. Maltez, L. Amaral, and M. Behar
Instituto de Física, Universidade Federal Rio Grande do Sul, 90501-970 Porto Alegre, Rio Grande do Sul, Brazil

A. Vantomme and G. Langouche
Instituut voor Kern-en Stralingsfysika, Catolic University, B-300L Leuven, Belgium

X. W. Lin
Lawrence Berkeley Laboratory, The University of California at Berkeley, Berkeley, California 94720
(Received 4 April 1996; revised manuscript received 16 July 1996)

The magnetic character and the ordering process of γ-$FeSi_2$ precipitates formed by Fe implantation into Si(100) followed by ion-beam epitaxial crystallization (IBIEC) have been studied using the Mössbauer technique. Measurements performed at 4 K have shown no evidence of magnetic interaction indicating that the γ-$FeSi_2$ phase is not of magnetic character. Conversely, conversion-electron Mössbauer experiments performed after the IBIEC procedure show basically the presence of a doublet, despite the cubic structure of the γ-$FeSi_2$ precipitates. However, after 1 h of annealing at 600 °C, a singlet, which before was barely recognizable, became more pronounced. The singlet-to-doublet proportion increases with increasing Fe concentration (2 at. $\% \leqslant C_p \leqslant 8.5$ at. %), indicating that after annealing a better ordering in the γ-$FeSi_2$ precipitates is achieved. This ordering is obtained by an adequate combination of Fe-implanted concentration and thermal annealing. These studies have been complemented by Rutherford backscattering and/or channeling and transmission electron microscopy experiments. [S0163-1829(96)07540-6]

I. INTRODUCTION

Recently, epitaxy of $FeSi_2$ on Si has attracted a great deal of attention because of its possible application in Si technology. As compared with other metal disilicides like $CoSi_2$ or $NiSi_2$, $FeSi_2$ is particularly interesting because it exists in four different phases denoted as α, β, pseudomorphic $FeSi_2$, and γ-$FeSi_2$ with distinct properties. The β-$FeSi_2$ is a semiconducting orthorhombic phase stable at temperatures below 950 °C. Optical and electronic spectroscopic[1] measurements have indicated that β-$FeSi_2$ has a direct transition with a band gap of about 0.85 eV, a feature that makes the β-$FeSi_2$ very attractive from the point of view of technical applications. The α-$FeSi_2$ is a metallic and tetragonal phase thermodynamically stable above 950 °C.[2] The newly discovered pseudomorphic $FeSi_2$ has been very recently produced by molecular-beam epitaxy on Si(111).[3] Its crystalline structure is of the Cl-Cs type with a random occupation of the Fe sites. It has been shown to be stable up to a temperature of ~500 °C, at which it transforms to the β-$FeSi_2$ phase.[3]

Despite the fact that the cubic γ-$FeSi_2$ phase has only recently been discovered, it has already been subject to extensive studies. The first reported γ-$FeSi_2$ phase was obtained either by molecular-beam epitaxy (MBE) combined with solid phase epitaxy[4] or by reactive deposition epitaxy[5] on a Si(111) substrate. The epitaxy of γ-$FeSi_2$ on Si(111) was also achieved by means of pulsed laser irradiation and subsequent ultrafast quenching of a thin β-$FeSi_2$ layer grown on top of a Si(111) substrate.[6] On the other hand, the γ-$FeSi_2$ phase has also been formed by using room-temperature Fe implantation and subsequent ion-beam-induced crystallization (IBIEC) of the Si(100) host.[7–10] A summary of all these studies has shown that the γ-$FeSi_2$ phase has a fluorite structure of metallic character with $a_c \cong a_{Si} = 0.543$ nm. It is a metastable phase that transforms to β-$FeSi_2$ at ~600–700 °C, the exact temperature being a function of the film thickness[4] or of the concentration of the implanted Fe.[10] A summary of the structure, lattice parameters, and general properties of the α, β, pseudomorphic, and γ-$FeSi_2$ phases is displayed in Table I.

In spite of the extensive work done in the characterization of the γ-$FeSi_2$ phase, several questions remain open, among them is its magnetic character. According to theoretical calculations[11] and Hall measurements,[4] the γ-$FeSi_2$ phase should be of magnetic character. Previous room-temperature Mössbauer experiments[12,13] have determined the existence of a doublet in the Mössbauer spectra, which has been interpreted in different ways. Fanciulli *et al.*[12] measured the Mössbauer spectrum corresponding to a thin γ-$FeSi_2$ film grown by a MBE technique on a Si(111) substrate. They fitted the experimental doublet with a sextet corresponding to an unusual low magnetic field. On the other hand, Desimoni *et al.*,[13] who performed Mössbauer measurements at room temperature and 17 K on γ-$FeSi_2$ samples prepared by the IBIEC technique, did not find any evidence of magnetic ordering. It should be stressed that despite the fluorite structure of the γ-$FeSi_2$ phase the Mössbauer spectra of Ref. 13 have not shown any evidence of a singlet, as would be expected from a cubic phase.

The above discussion shows that at least two questions are still left open. First, is γ-$FeSi_2$ a magnetic phase? Second, if it is not a magnetic one, why does the characteristic singlet not appear in the Mössbauer spectrum despite its cubic character?

TABLE I. Structure, lattice parameters, and general properties of the α, β, pseudomorphic, and γ-$FeSi_2$ phases.

		Lattice parameters (Å)			
Phase	Structure	*a*	*b*	*c*	Properties
β-$FeSi_2$	Orthorhombic	9.86	7.79	7.83	*Stable*<≈950 °C Semiconducting
α-$FeSi_2$	Tetragonal	2.695		5.13	*Stable*>≈950 °C metallic
Pseudomorphic-$FeSi_2$	ClCs	~2.7			Metastable ~500 °C
γ-$FeSi_2$	CaF_2	≈5.43			*Metastable*<700 °C Metallic

The present work was undertaken in order to answer the above-mentioned questions. With this purpose in mind ^{57}Fe was implanted into the Si(100) matrix and subsequently the IBIEC procedure was carried out. In a first stage and looking for the possible magnetic character of the γ-$FeSi_2$ phase, Mössbauer data were collected at 4 K in a transmission geometry. Then, we studied the ordering of the γ-$FeSi_2$ phase as a function of the Fe concentration and the different thermal treatments to which the samples were submitted. At each stage of this second set of experiments, Mössbauer measurements (in a backscattered geometry) were performed and the evolution of their hyperfine parameters was followed in order to determine its dependence on the Fe concentration and thermal treatments. These last studies have been complemented by Rutherford backscattering and/or channeling and transmission electron microscopy experiments.

II. EXPERIMENTAL PROCEDURE

Si(001) wafers (p type with a resistivity of 1 Ω cm) were ^{57}Fe implanted at room temperatures at 50 keV. Several fluences were used in order to obtain Fe peak concentrations ranging between 2 and 8.5 at. %. Beam heating was minimized by keeping the beam flux below 1 μA cm^{-2}; channeling effects were minimized by tilting the wafer normal 7° away from the beam direction. The implantation-induced amorphous layer was subsequently crystallized by the IBIEC process. With this aim the samples were irradiated at 320 °C with 380-keV Ne ions.

The Mössbauer transmission experiments at 4 K were performed using a helium-bath cryostat system. A 25-mCi ^{57}CoRh source was used to obtain the 14.4-keV γ ray from ^{57}Fe. The conversion-electron Mössbauer (CEMS) experiments were carried out at room temperature in a conventional constant acceleration spectrometer. The conversion electrons coming from the absorber sample were detected with a He-methane gas (6%) flux detector. All data analyses were performed using a nonlinear least-squares-fit routine developed in our laboratory.[14]

Subsequent thermal annealings were performed at temperatures ranging between 600 and 900 °C in a vacuum better than 10^{-7} Torr. The annealing times were varied between 1 and 24 h. At different stages of the experiments the samples were analyzed by Rutherford backscattering and/or channeling spectroscopy (RBS/C) with a He^{2+} beam at 800 keV in a 165° scattering geometry. The overall resolution of the detector plus electronic system was better than 13 keV.

In addition, the specimen structure was characterized by using cross-sectional transmission electron spectrometry (TEM) including selected area diffraction (SAD) and high-resolution electron microscopy (HREM). TEM specimens were prepared by mechanical polishing and ion milling.

The ^{57}Fe implantations were performed at Leuven using the 100-keV mass separator. The IBIEC, RBS/C, and CEMS experiments were done at Porto Alegre. Finally the TEM experiments were performed at the Lawrence Berkeley Laboratory using the JEOL 200 CX high resolution microscope.

III. EXPERIMENTAL RESULTS

A. As implanted and IBIEC samples

Figure 1 shows the random and channeled RBSC spectra after Fe implantation of the Si(100) sample with a 5×10^{15} at/cm^2 fluence (C_p=2 at. %). The Si wafer is amorphized over 100 nm and no channeling was observed in the Fe signal. Figure 2 shows that after the subsequent IBIEC procedure the entire amorphous layer is recrystallized, the minimum backscattering yield on the subsurface region being

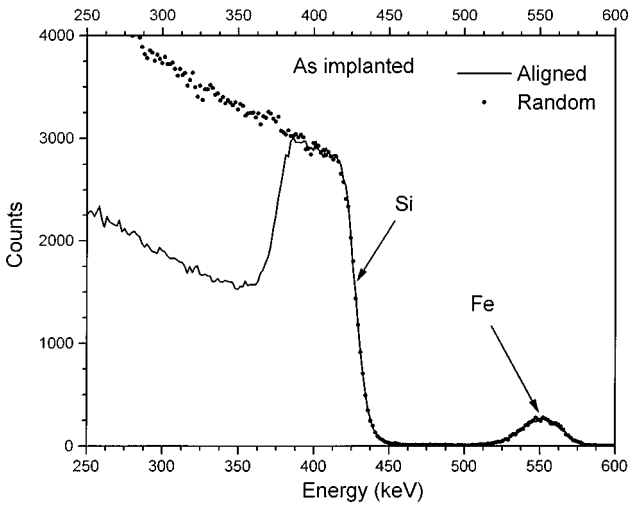

FIG. 1. Random (circles) and channeled RBSC spectra (full line) of Si(100) sample implanted with 50-keV Fe at a fluence $\phi=5\times10^{15}$ at cm^2.

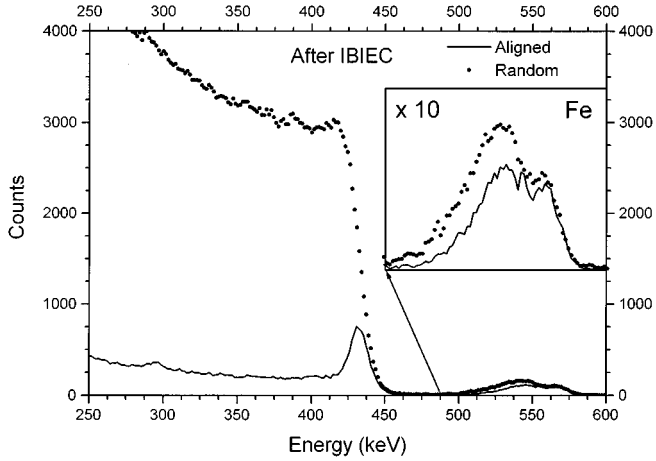

FIG. 2. Same as Fig. 1 after the IBIEC procedure—see text. The Fe profile shows a partial degree of alignment and the Si have been completely recrystallized.

χ_{min}=8%. The Fe peak shows a small segregation toward the surface and a moderate channeling (χ_{min}=65%). Previous TEM studies performed on similar IBIEC-treated samples[10] show that as a consequence of this procedure predominantly *A*-type cubic γ-$FeSi_2$ precipitates are formed (70% of the total amount). This kind of precipitate is fully aligned with the Si matrix, at variance with the *B*-type precipitates, which are twinned with respect to the *A* type.

B. Low-temperature Mössbauer results

In Fig. 3 the transmission Mössbauer spectrum of a 2-at. % sample after the IBIEC procedure (as-IBIEC sample) at 4 K is shown. As can be observed, it definitively does not show the characteristic sextet typical of a magnetic interaction. Rather, it consists of an asymmetric doublet, quite similar to the one obtained at room temperature and therefore adjusted with the same fitting procedure (considering a quadrupole interaction plus a singlet), as will be discussed in Sec. III C.

C. Room-temperature Mössbauer results

Figure 4(a) shows the CEMS spectrum of the 2-at. % as-IBIEC sample. It again consists of an asymmetric doublet

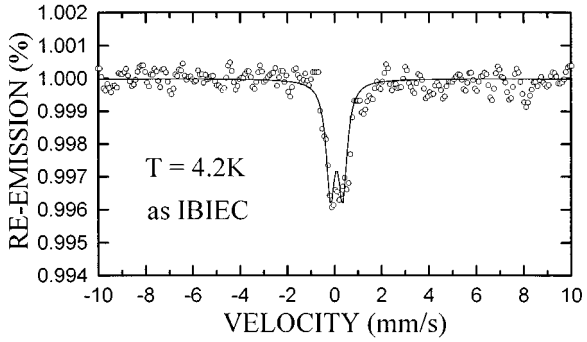

FIG. 3. Mössbauer spectrum for C_p=2 at. % after IBIEC is taken at 4 K in a transmission geometry.

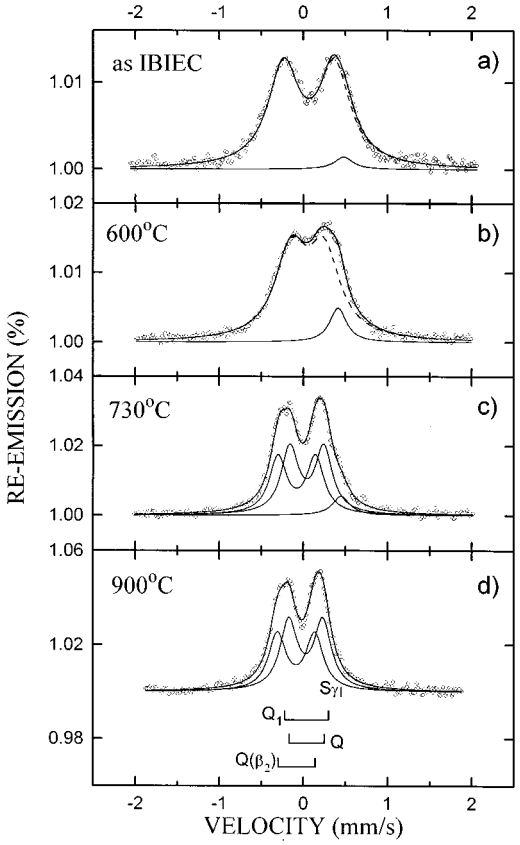

FIG. 4. CEMS spectra for C_p=2 at. % Fe implanted sample: (a) after the IBIEC procedure; (b) same as (a) after subjecting the sample to 600 °C, 1-h annealing; (c) same as (a) after subjecting the sample to 1-h, 730 °C annealing; (d) same as (a) after subjecting the sample to 1-h, 900 °C annealing.

that was fitted basically with one quadrupole interaction of Q_1=0.26±0.03 mm/s and δ=0.04±0.02 mm/s and the singlet $S\gamma$ that is characterized by the isomer shift δ=0.45 ±0.03 mm/s. The hyperfine parameters are displayed in Table II and the normalized CEMS spectral areas (in %) are shown in Table III(a). The 1-h thermal annealing at 600 °C induces significant changes in the CEMS spectra, as revealed by Fig. 4(b). The doublet becomes narrower and slightly asymmetric. Consequently the quadrupole interaction *Q* diminishes (Q=0.21±0.03 mm/s), but the singlet remains at the same isomer shift. On the other hand, the singlet-to-doublet proportion increases (beyond the experimental error) as shown in Table III(a).

TABLE II. ^{57}Fe Mössbauer parameters obtained from the least-squares fit to the present data. $S\gamma$, Q_1, Q, and $Q(\beta_2)$ are the singlet and the corresponding quadrupole splitting—see text.

	ΔE_Q (mm/s)	δ (mm/s)	Γ (mm/s)
$S\gamma$		0.45±0.03	0.30±0.05
Q_1	0.26±0.03	0.04±0.02	0.40±0.05
Q	0.21±0.03	0.04±0.02	0.30±0.05
$Q(\beta_2)$	0.22±0.01	−0.08±0.01	0.25±0.05

TABLE III. (a) Normalized CEMS spectral areas (in %) as obtained in the present experiment (typical errors ±2%). As IBIEC means immediately after the IBIEC process, while 600 °C, 730 °C, and 900 °C mean the annealing temperatures to which the samples were subjected after the IBIEC process—see text. (b) Normalized spectral area (in %) obtained for different Fe peak concentrations after the IBIEC process (typical errors ±2%). In addition, we show the same areas after the 1-h 600 °C anneal process.

(a)

T (°C)	$S\gamma$	Q_1	Q	$Q(\beta_2)$
as IBIEC	5	95		
600	10		90	
730	5		52	43
900			55	45

(b)

	as IBIEC		600 °C/1 h		
C_P^{Fe} (%)	$S\gamma$	Q_1	$S\gamma$	Q	$Q(\beta_2)$
2	5	95	10	90	
4	5	95	20	69	11
5.5	5	95	9	58	33
8.5	5	95	5	52	43

The RBSC measurements done on the 2-at. % sample after the annealing at 600 °C reveal that the χ_{min} of the Fe part of the spectrum improves, reaching a value of 55%—see Table IV. Hence, both the CEMS and RBSC experiments indicate that after the thermal annealing the ordering of the γ-$FeSi_2$ precipitates has improved. However, subsequent annealings performed up to 24 h at 600 °C have not changed further the experimental situation.

The annealing performed at 730 °C for 1 h induces a drastic change in the shape of the doublet, as shown in Fig. 4(c). The CEMS spectrum is now fitted with the singlet $S\gamma$ and the two quadrupole interactions Q and $Q(\beta_2)$ characteristics of the β-$FeSi_2$ phase[15]—see Table II. In addition, RBSC experiments show the complete absence of alignment, in agreement with previous results obtained with similarly treated samples.[10] Further annealing at 900 °C for 1 h induces the disappearance of the singlet $S\gamma$ in the CEMS spectrum leaving only the two doublets Q and $Q(\beta_2)$ as displayed in Table III(a).

In a next step we have changed the Fe peak concentration C_p in the Si-implanted samples from 4 up to 8.5 at. %. The CEMS spectra recorded for the 4-, 5.5-, and 8.5-at. % samples after the IBIEC procedure were all quite similar to the one obtained for the 2-at. % sample. They were all analyzed with the same hyperfine parameters, and in all the cases the same singlet-to-quadrupole interaction proportion was obtained—see Table III(b).

TABLE IV. χ_{min} values for the Fe part of the RBSC spectra for different Fe peak concentrations, obtained after the IBIEC process and subsequent 1-h 600 °C anneal, respectively.

	χ_{min}^{Fe} (%)	
C_P (%)	as IBIEC	600 °C/1 h
2	65	55
4	75	82
5.5	80	92
8.5	⩾95	>95

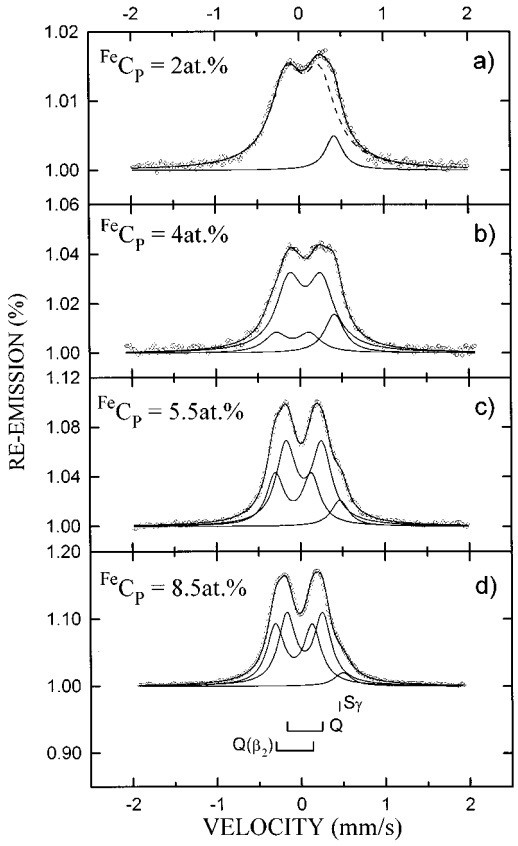

FIG. 5. CEMS spectra obtained after 1 h annealing at 600 °C for samples with different Fe concentration. (a) C_p=2 at. %; (b) C_p=4 at. %; (c) C_p=5.5 at. %; and (d) C_p=8.5 at. %.

However, the subsequent 1-h annealing at 600 °C on the three samples has drastically induced different effects, as can be deduced by observation and analysis of the corresponding Mössbauer spectra—see Figs. 5(b)–5(d). The CEMS spectrum corresponding to the 4 at. % sample was fitted with the singlet $S\gamma$ and the two doublets Q and $Q(\beta_2)$, the proportions being 20%, 69%, and 11%, respectively, as quoted in Table III(b). The corresponding RBSC spectrum indicates that the χ_{min} of the Fe signal has increased from 75% (after the IBIEC procedure) up to 82% after the 1-h annealing—see Table IV. The analysis of the Mössbauer spectra corresponding to the 5.5-at. % sample shows the same features and is fitted with the same parameters $S\gamma$, Q, and $Q(\beta_2)$, but with different proportions: 9%, 58%, and 33%, respectively [Table III(b)]. The original χ_{min} for the as-IBIEC sample has increased from 80% to 92% (Table IV). Finally the analysis of the CEMS spectra corresponding to the 8.5-at. % sample reveals that after 1 h annealing the Mössbauer spectrum was basically fitted with the two doublets Q and $Q(\beta_2)$, leaving only a small proportion of the $S\gamma$ singlet [Table III(b)]. In this case the original χ_{min} is almost 100%, so the subsequent annealing did not introduce significative changes.

IV. DISCUSSION

Previous works[7–10] have shown that cubic γ-$FeSi_2$ precipitates are formed whenever Fe is implanted into a Si(100) matrix and subsequently submitted to an IBIEC procedure. For low implanted Fe concentrations ($C_p \leqslant 5$ at. %), the *A* type is predominant. However, when C_p is increased, three features are observed: (a) there is an increase in the size of the precipitates, (b) a decrease in their density, and (c) a gradual transformation in their orientation from *A* to *B* type. In addition it has been shown that the γ-$FeSi_2$ phase is metastable and transforms into β-$FeSi_2$ upon thermal annealing. The transformation temperature was determined as $T \approx 700$ °C for $C_p = 2$ at. %. However, for higher Fe concentrations evidence exists that this temperature decreases.[16]

As was mentioned in the Introduction, theoretical calculations[11] and Hall[4] measurements indicated that the γ-$FeSi_2$ phase should be of magnetic character. However, Desimoni *et al.*,[13] by performing Mössbauer experiments at 17 K, did not find evidence of magnetic ordering. In the present work, Mössbauer measurements were performed at 4 K and still at this very low temperature no evidence of magnetic splitting was found in the Mössbauer spectrum. Then, we can conclude the γ-$FeSi_2$ phase is of nonmagnetic character. The apparent discrepancy with the Hall measurements could in principle be attributed to the interpretation of these last results, an interpretation that is less straightforward than the one obtained from the present experiments.

On the other hand, early Mössbauer measurements performed at room temperature[13] (done with samples similar to the ones used in the present study) resulted in CEMS spectra that were fitted with only quadrupole doublets. In spite of the fluorite structure of the γ-$FeSi_2$ phase no significant evidence of a singlet was observed. It was argued[13] that displacements of the Fe atoms and/or vacancies in the Fe sublattice could be responsible for the appearance of the quadrupole interaction and the absence of the singlet. If this is the case, it can be expected that by increasing the Fe concentration and/or subjecting the samples to thermal annealing, it should be possible to achieve improvement in the ordering of the Fe sublattices. Consequently, this feature should be reflected in the Mössbauer spectra with the appearance of the singlet characteristic of a cubic ordered structure. A very similar CEMS spectrum of an MBE-deposited γ-$FeSi_2$ layer has been interpreted as an unresolved magnetically split sextet.[12] It should be stressed that in this case no further improvement of the cubic structure can be achieved since both an increase of the thickness as well as thermal annealing result in a prompt γ-$FeSi_2$ to β-$FeSi_2$ phase transition.

In the present work, the CEMS spectra of the $C_p = 2$ at. % sample after the IBIEC procedure already show the presence of a singlet; however, only in a very small proportion. The subsequent annealing at 600 °C increases this fraction to 10%. In addition, the RBSC measurements show that the $\chi_{\min}$ corresponding to the Fe part of the RBS spectrum has improved from 65% to 55%. Both features are clear evidence of a better ordering in the γ-$FeSi_2$ precipitates, which is induced by the thermal treatment of the sample. This behavior has been confirmed by TEM observations,[17] which have shown that the annealing performed after the IBIEC procedure completes the formation of γ-$FeSi_2$ precipitates starts a coarsening process and consequently improves the crystallinity of the sample.

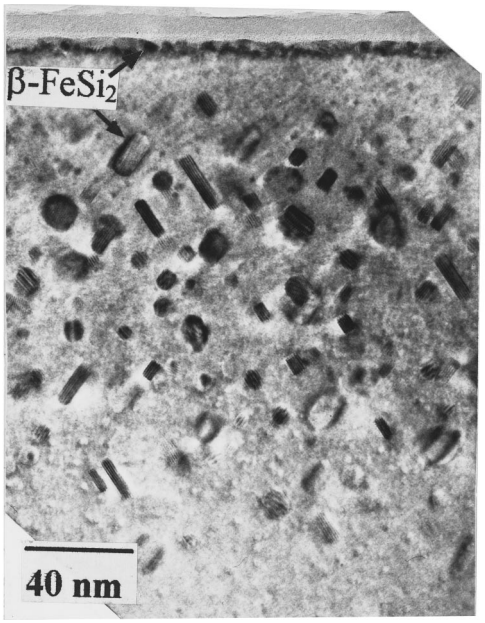

FIG. 6. Cross-sectional TEM micrograph of Fe-implanted Si ($C_p = 2$ at. %) sample after IBIEC process and after 730 °C annealing for 30 min. Note the surface layer (~6 nm thick) consisting of β-$FeSi_2$ precipitates. The region immediately below this layer is ''dilute'' in precipitates. At the deeper region there is a broad distribution of β and γ precipitates.

The thermal annealing at 730 °C on the same sample induces a massive γ-to-β phase transformation, as illustrated by TEM experiments. Figure 6 shows a TEM micrograph of a similar $C_p = 2$ at. % sample, which was annealed at 730 °C. A near surface layer (about 6 nm thick) of β-$FeSi_2$ is separated from a broad distribution of β and γ precipitates extending from a depth of 25 nm towards the bulk. Furthermore, TEM observations show that with increasing temperature the number of β-$FeSi_2$ precipitates increases and that finally at 900 °C the γ-to-β phase transformation is almost completed.

The present Mössbauer results are completely consistent with the TEM observations. The CEMS spectrum recorded after the 730 °C annealing was fitted with hyperfine parameters [$S\gamma$, Q, and $Q(\beta_2)$] that revealed the coexistence of both γ and β phases. Finally, after annealing at 900 °C the corresponding CEMS spectrum was fitted with the two doublets Q and $Q(\beta_2)$ characteristic of the β-$FeSi_2$ phase in the proportion (55% and 45%, respectively) reported in the literature.[15]

At this point we want to discuss the Mössbauer parameters characteristic of the γ and β-$FeSi_2$ phases that appear in the present experiment. As an example, we consider the $C_p = 2$ at. % sample. After the 1-h annealing at 600 °C, only the γ phase is present, resulting in the Mössbauer parameters $S\gamma$ and Q. On the other hand, after the 900 °C annealing, basically only the β phase is present and the corresponding hyperfine parameters are Q and $Q(\beta_2)$. Therefore, it should be concluded that the Q doublet is not only characteristic of the β phase but also of the γ phase. The individual phases can be distinguished by the appearance of either the singlet

TABLE V. (a) CEMS spectral areas (in %) for the γ and β-$FeSi_2$ phases, as deduced from the analysis of Table III(a)—see text. (b) CEMS spectral areas (in %) for the γ and β-$FeSi_2$ phases, as deduced from the analysis of Table III(b)—see text.

(a)

T (°C)	γ-$FeSi_2$ $S\gamma$	$Q(\gamma)$	β-$FeSi_2$ $Q(\beta_1)$	$Q(\beta_2)$
600	10	90		
730	5		52	43
900			55	45

(b)

600 °C/1 h

	γ-$FeSi_2$			β-$FeSi_2$	
C_P^{Fe} (%)	$S\gamma$	$Q(\gamma)$	$S\gamma/Q(\gamma)$	$Q(\beta_1)$	$Q(\beta_2)$
2	10	90	0.11		
4	20	56	0.36	13	11
5.5	9	18	0.50	40	33
8.5	5		Only $S\gamma$	52	43

$S\gamma$ for the γ phase or the doublet $Q(\beta_2)$ for the β phase.

In order to extract from the Mössbauer experiments for the $C_p=4$, 5.5, and 8.5 at. % cases the proportions in which the γ and β phases appear, one should make two assumptions, namely: (a) The Q doublet represents two contributions $Q(\gamma)$ and $Q(\beta_1)$, characteristic of the γ and β phases, respectively; and (b) the ratio between the doublets characteristic of the β phase $r=Q(\beta_1)/Q(\beta_2)$ is $r=1.2$, as quoted by the literature[15] and observed in the present work.

Taking into account the above assumptions, it is possible to extract from Tables III(a) and III(b) the normalized CEMS spectral areas corresponding to each phase at each stage of the experiment. The γ-$FeSi_2$ phase is characterized by the singlet $S\gamma$ and the doublet $Q(\gamma)$, and the β-$FeSi_2$ phase by the pair of doublets $Q(\beta_1)$ and $Q(\beta_2)$. The corresponding values for the 2 at. % concentration at the different annealing temperatures and the ones for the different concentrations after 1 h annealing at 600 °C are displayed in Tables V(a) and V(b), respectively.

Table V(a) shows that a phase transformation has already occurred at 730 °C. The γ-phase contribution is 5%, while the one corresponding to the β phase is 95%. These proportions are consistent with the TEM observations,[10] which, as discussed above, have shown that at this temperature a massive γ-to-β phase transformation occurs.

From Table V(b) several interesting features become clear. First, the contribution of the γ-$FeSi_2$ phase decreases with increasing Fe concentration from 100% for $C_p=2$ at. % down to 5% for $C_p=8.5$ at. %. This behavior can be understood if one considers the mechanism of the γ-to-β phase transformation, which involves two factors: (i) the size of the precipitates, which depends on the implanted Fe concentration; and (ii) the coalescence process induced by the thermal annealing. As was shown previously,[17] a phase transformation occurs whenever the γ-$FeSi_2$ precipitates reach a critical size (around 10 nm) induced by the coalescence mechanism. Therefore both factors, the implanted Fe concentration and the corresponding temperature for the phase transformation, are expected to be strongly related each other. The higher the Fe concentration, the lower the temperature of transformation should be. This behavior is what we observe in the present experiment. The γ-to-β phase transformation is induced at 730 °C when the Fe concentration is $C_p=2$ at. %, but this temperature decreases to 600 °C when $C_p\geqslant 4$ at. %, indicating that the contribution of the β phase is strongly related to the implanted Fe concentration.

It should be stressed that the RBSC observations are consistent with the above considerations. As can be observed from inspection of Table IV the $\chi_{\min}$ of the Fe part of the RBSC spectra for $C_p\geqslant 4$ at. % increases after the annealing is performed at 600 °C. This behavior is consistent with an increasing presence of the β phase as revealed by the CEMS experiments.

In addition, when paying attention to the behavior of the γ-$FeSi_2$ phase, it is observed that $S\gamma/Q(\gamma)$ ratio increases with increasing concentration, starting from 0.11 for $C_p=2$ at. %, up to 0.5 for $C_p=5.5$ at. %. Finally for $C_p=8.5$ at. % the singlet is the only contribution to the γ-$FeSi_2$ phase. This behavior confirms our previous assumptions about the ordering of the γ-$FeSi_2$ phase as a function of the temperature and the implanted Fe concentration. In fact, after the IBIEC process the singlet-to-doublet ratio was independent of the implanted concentration. However, the annealing performed at 600 °C not only improved the ordering of the precipitates but also revealed the strong dependence of the singlet contribution with the implanted Fe concentration.

We would like to speculate on the mechanism responsible for the increasing $S\gamma/Q(\gamma)$ ratio with increasing Fe concentration (after the annealing procedure). The $S\gamma$ singlet is associated with a perfect cubic structure and the doublet $Q(\gamma)$ with a nonperfect one. If it is assumed that in the bulk of the precipitates the structure is ordered, but near the γ-$FeSi_2$/Si interface there are imperfections that introduce disorder, then the $S\gamma$ signal should arise from the bulk and the $Q(\gamma)$ from the interface region. At low Fe concentrations the precipitates are small and so is the volume-to-surface ratio. Then, it is expected that the $S\gamma/Q(\gamma)$ ratio should be also small. On the other hand, with increasing Fe concentration, the size of the precipitates increases, and so does the volume to surface ratio. Then it is expected that the $S\gamma/Q(\gamma)$ ratio become larger. In fact, this is exactly what was observed when the Fe concentration was increased from 2 up to 8.5 at. %.

V. CONCLUSIONS

The results of the present work clearly show that the γ-$FeSi_2$ phase is of nonmagnetic character. This feature is revealed by the Mössbauer experiments performed at 4 K, which do not reveal any magnetic splitting in the corresponding Mössbauer spectra.

In addition, the present experiments show several interesting features of the ordering of the γ-$FeSi_2$ phase as a function of the implanted Fe concentration and the annealing temperature of the system. The precipitates, as formed by the IBIEC process, are highly disordered, with the degree of disorder being independent of the implanted Fe concentration. This situation changes drastically after annealing for 1 h at 600 °C. It is shown that the ordering is strongly correlated to the implanted concentration, as revealed by the singlet-to-doublet ratio in the corresponding Mössbauer spectra. This ratio increases with increasing concentration, indicating an ordering process within the γ-$FeSi_2$ precipitates. Very likely,

this behavior occurs due to the growing process of the precipitates, as discussed in the preceding section. However, there is a concentration limit ($C_p \approx 8$ at. %) for the ordering process, a concentration at which a nearly complete γ-to-β phase transformation is observed. Nevertheless, at this concentration, a trace of the singlet is still observed, indicating that at this critical concentration the γ-$FeSi_2$ precipitates that have survived are completely ordered in their cubic phase.

[1] N. Cherief, C. D'Anterroches, R. C. Cinti, T. A. Nguyen Tan, and J. Derrien, Appl. Phys. Lett. **55**, 1671 (1989).

[2] U. Birkholz and J. Schelm, Phys. Stat. Solidi **34**, K177 (1969).

[3] H. Sirringhaus, N. Onda, E. Müller-Gubler, P. Müller, R. Stalder and H. von Känel, Phys. Rev. B **47**, 10 567 (1994).

[4] N. Onda, J. Henz, E. Müller, K. A. Mäder and H. von Känel, Appl. Surf. Sci. **56-58**, 421 (1992).

[5] V. Le Thanh, J. Chevrier, and J. Derrien, Phys. Rev. B **46**, 15 946 (1992)

[6] M. G. Grimaldi, P. Baeri, C. Spinella, and S. Lagomarsino, Appl. Phys. Lett. **60**, 1137 (1992).

[7] J. Desimoni, H. Bernas, M. Behar, X. W. Lin, J. Washburn and Z. Liliental-Weber, Appl. Phys. Lett. **62**, 306 (1993) .

[8] X. W. Lin, M. Behar, J. Desimoni, H. Bernas, J. Washburn, and Z. Liliental-Weber, Appl. Phys. Lett. **63**, 105 (1993).

[9] R. L. Maltez, M. Behar, L. Amaral, P. F. P. Fichtner, and X. W. Lin, Nucl. Instrum Methods Phys. Res. B **96**, 366 (1995).

[10] M. Behar, H. Bernas, J. Desimoni, X. W. Lin, and R. L. Maltez, J. Appl. Phys. **79**, 752 (1996).

[11] N. E. Christiansen, Phys. Rev. B **42**, 7148 (1990).

[12] M. Fanciulli, G. Weyer, H. von Känel, and N. Onda, Phys. Scr. **T54**, 16 (1994).

[13] J. Desimoni, F. H. Sanchez, M. V. Ferandez van Raap, H. Bernas, C. Clerc, and X. W. Lin, Phys. Rev. B **51**, 86 (1995).

[14] L. Amaral, Ph.D. thesis, Universidade Federal Rio Grande de Sul, 1984 (unpublished).

[15] R. Wandji, Phys. Stat. Solidi B **45**, K123 (1971).

[16] X. W. Lin (private communication).

[17] X. W. Lin, J. Washburn, Z. Liliental-Weber, and H. Bernas, J. Appl. Phys. **75**, 4686 (1994).